A First-Principles Based Approach to Potential Attenuation Projection for Marine Pipelines and Risers

W.H. Hartt and D.K. Lysogorski
Center for Marine Materials
Department of Ocean Engineering
Florida Atlantic University – Sea Tech Campus
101 North Beach Road
Dania Beach, Florida 33004 USA

Abstract

Cathodic protection (cp) design and analysis tools for one dimensional systems such as pipelines and risers are reviewed with emphasis being given to newly proposed, first-principles based potential attenuation and anode/anode bed current output equations that incorporate all relevant resistance terms (anode (electrolyte), coating, polarization, and metallic path). One of the new expressions pertains to pipelines with superimposed (bracelet) anodes and a second to the case where the anode/anode bed is offset from the pipeline, as occurs for buried onshore pipelines and marine pipeline cp retrofits and pipelines deployed by reeling. In effect, the former (superimposed anode) is a special case of the latter. It is demonstrated that the expressions can be employed to analyze both galvanic and impressed current cp systems. Comparisons are made between the potential attenuation projected by the present expression and by the classical equations of Morgan/Uhlig. It is concluded that the Morgan/Uhlig approach is non-conservative in cases where the pipeline, or a portion thereof, lies within the anode potential field.

Key words: Pipelines, cathodic protection, potential attenuation, design

Introduction

Submerged and buried pipelines are invariably protected from external corrosion by a combination of coatings and cathodic protection (cp). In effect, the cp provides protection per se while the coating system renders the cp more efficient and effective. This results because the coating reduces the effective exposed pipe surface area such that cp is needed only at coating defects. Consequently, pipe current demand to achieve a requisite polarization is reduced, thereby lowering anode output requirements and increasing the spacing between anodes or anode ground beds. Cathodic protection systems for marine compared to buried onshore pipelines are distinctive in several regards. Thus, design in the former case normally assumes several percent coating bare area and employs galvanic bracelet anodes spaced about 250 m apart. This relatively short spacing arises because of, first, limitations on the size of bracelet anodes that can be deployed from a lay barge and, second, the fact that current density demand is relatively high and service lives of 20-30 years are needed. For the on-shore buried counterpart, on the other hand, higher coating quality combined with impressed current (ic) cp, which is the type normally employed here, is such that metallic path ground return resistance is the controlling factor; and, consequently, anode ground bed spacings as great as 50-100 km can be realized. Figure 1 schematically shows the potential profile that results in each of these two cases. Thus, for the galvanic bracelet anode situation (Figure 1a) potential is constant except within the field of the anode which normally extends only about 10-15 m. Here, the magnitude of pipe polarization is determined by electrolyte resistivity, anode dimensions, and anode current output (alternatively, pipe current demand). Buried pipelines with iccp and large anode/anode bed spacings, on the other hand, exhibit continued polarization decay with increasing distance beyond the field of the anode (Figure 1b) in conjunction with the voltage drop in the pipeline. As such, generalized pipeline polarization

behavior reflects influences from four resistance terms; the anode (electrolyte), coating, electrochemical polarization, and metallic path return. The critical design parameter in the galvanic anode (ga) cp case is projection of pipe current demand. For buried pipelines with iccp, anode ground bed design and spacing are also important.

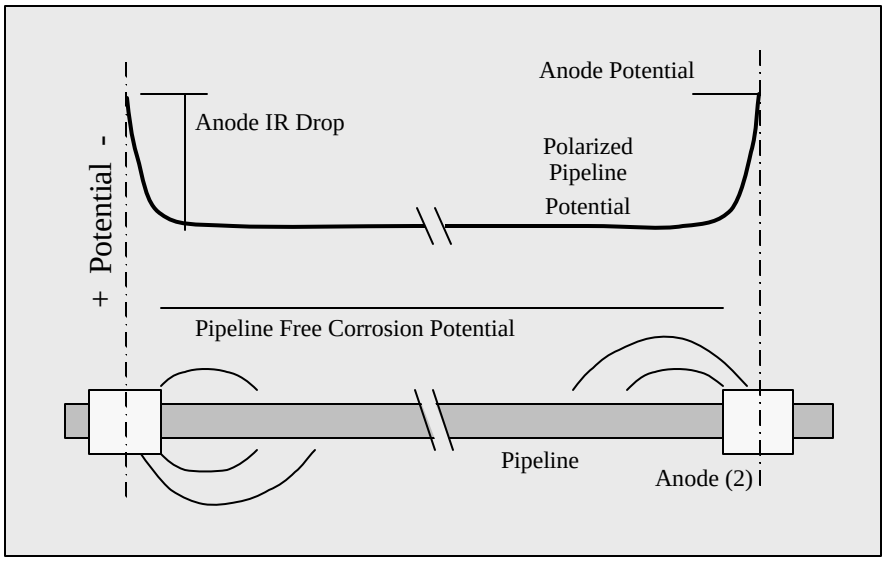

(a)

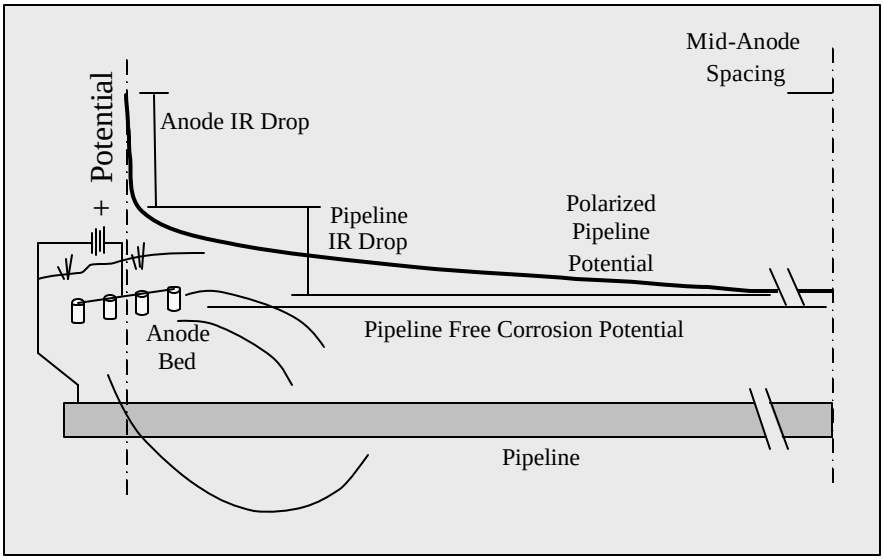

(b)

Figure 1: Schematic illustration of potential profiles that arise from (a) galvanic cp of marine pipelines with bracelet anodes and (b) impressed current cp of buried pipelines.

Pipeline Cathodic Protection Design

For marine pipelines with closely spaced galvanic anodes such that metallic path resistance is negligible, the design process has historically involved the following steps [1,2]:

1. Calculation of net pipe current demand, I_c, from the expression,

$$I_c = A_c \cdot f_c \cdot i_c, \quad (1$$

where A_c is the pipe surface area, f_c the coating breakdown factor (ratio of bare to total pipe surface area), and i_c is current density demand (normally specified for marine applications as 60-170 mA/m^2 (bare surface area basis)) [1,2] depending upon water depth, temperature, sea water versus mud exposure, and whether or not the calculation is for the mean ($i_c = i_m$) or final ($i_c = i_f$) condition, where i_m is the time-averaged current density and i_f is the current density near the end of the design life.

2. Determination of the net anode mass, M (kg), from a modified form of Faraday's law,

$$M = \frac{8{,}760 \cdot i_m \cdot T}{u \cdot C}, \quad (2$$

where u is a utilization factor, C is current capacity (kg/A-y), and T is design life (y) and of current output of individual anodes, I_a, from Ohm's law,

$$I_a = \frac{f_c - f_a}{R_a}, \quad (3$$

where f_c and f_a are the closed circuit pipe and anode potentials, respectively, and R_a is anode resistance. For bracelet anodes, R_a is normally calculated using McCoy's formula [3],

$$R_a = \frac{0.315 \cdot r_e}{\sqrt{A_a}}, \quad (4$$

where r_e is electrolyte resistivity and A_a is anode surface area.

3. Lastly, the number of anodes, N, is determined as,

$$N = \frac{I_c}{I_a}. \quad (5$$

For 1) marine pipeline cp retrofits, 2) marine pipelines deployed by reeling with subsequent anode sled placement, and 3) buried onshore pipelines with iccp systems, anode spacing is likely to be large and metallic path resistance significant, as discussed above. For this circumstance, the classical first-principles based equations of Morgan [4] and Uhlig [5] are useful. Thus, for pipelines polarized by identical, equally spaced anodes,

$$E_z = E_b \cdot \cosh\left[\left(\frac{2\pi r_p \cdot R_m}{k \cdot z}\right)^{1/2} \cdot \left(z - L_{as}/2\right)\right] \text{ or}$$

$$E_a = E_b \cdot \cosh\left[-\left(\frac{2\pi r_p \cdot R_m}{k \cdot z}\right)^{1/2} \cdot L_{as}/2\right], \quad (6$$

where

E_a, E_b, and E_z are the magnitudes of polarization at the drainage point, the mid-anode spacing, and at distance z from a drainage point,

r_p is the pipe radius,

R_m the pipe electrical resistance per unit length,
$k \cdot z$ the current density demand, and
L_{as} the anode spacing.

Difficulties here, however, are that, first, anode resistance does not appear explicitly and, second, there is uncertainty associated with E_a, E_b and $k \cdot z$. Numerical methods such as Boundary Element Modeling (BEM) incorporate anode resistance and accommodate the fact that f_c is a function of z; however, they do not consider metallic path resistance.

Newly Proposed Attenuation Equations

Pipelines Protected by Superimposed (Bracelet) Anodes: Pierson et al. [6] and Lysogorski et al. [7] improved upon the Morgan/Uhlig expression by introducing the governing equation,

$$E_c''(z) = U_m''(z) - U_e''(z), \quad (7$$

where, $U_e(z)$ and $U_m(z)$ are potentials in the metallic pipe and electrolyte, respectively, at distance z along the pipeline from the centerline of an anode, these being superimposed on the pipe, identical, and equally spaced. The former term was evaluated as,

$$DU_e = I_e(z) \cdot R_e(Dz), \quad (8$$

where $I_e(z)$ is current in the electrolyte at z and $R_e(Dz)$ is the incremental resistance difference between two successive nodes in the electrolyte. The $E_c(z)$ term was addressed by assuming a linear relation between f_c and i_c according to,

$$E_c(z) = a \cdot g \cdot i_c(z), \quad (9$$

where,

a is the polarization resistance and
g is the total-to-bare pipe surface area ratio ($1/f_c$).

Substitution of this and a modified version of the differential equation that yielded Equation 6 [4,5],

$$U_m''(z) = \frac{R_m \cdot 2 \cdot p \cdot r_p}{a g} \cdot E_c(z), \quad (10$$

into Equation 7 yielded what has been termed an inclusive attenuation equation for polarization of a uni-dimensional system,

$$E_c''(z) + \left(\frac{H}{z^2} + B \right) \cdot E_c(z) = \frac{2 \cdot H}{z^3} \int_z^{L_{as}/2} E_c(t) \cdot dt, \quad (11$$

where $E_c(z)$ is the magnitude of pipe polarization at z, $H = \frac{r_e \cdot r_p}{a \cdot g}$, $B = \frac{-R_m \cdot 2 \cdot p \cdot r_p}{a \cdot g}$, and r_e is electrolyte resistivity. The expression is distinct compared to Equation 6 in that coating, polarization, and metallic path return resistances are included explicitly and anode (electrolyte) resistance implicitly as the integral term, whereas Equation 6 does not include the anode resistance term and numerical modeling the metallic path. Together, the

product of a and g is synonymous with $k \cdot z$ from the Uhlig expression. Table 1 provides a comparison between $a \cdot g$ and the more conventional representation of pipe current density demand in terms of f_c and i_c.

Table 1: Listing of a range of ag values as related to coating quality (g and f_c) and i_c.

Pipe Bare Area, percent	f_c	g	i_c, mA/m^2	a, Ωm^2*	ag, Ωm^2
0	0	8	5	70	∞
			20	10	
			50	7	
0.01	0.0001	10,000	5	70	700,000
			20	10	100,000
			50	7	70,000
0.1	0.001	1,000	5	70	70,000
			20	10	10,000
			50	7	7,000
1	0.01	100	5	70	7,000
			20	10	1,000
			50	7	700
5	0.05	20	5	70	1,400
			20	10	200
			50	7	140
100	1	1	5	70	70
			20	10	10
			50	7	7

* This parameter was calculated, assuming a linear cathodic polarization curve, as the slope corresponding to the indicated i_c at 0.35 V polarization.

Equation 11 has been solved using a Coordinate Mapping Based Finite Difference Method (CoMB-FDM) numerical procedure. In so doing, an anode was positioned at $z = 0$; and the initial pipeline numerical increment, Dz, was set equal to the radius of a spherical anode, $r_a(eq)$, the resistance of which is the same as that of a bracelet anode based upon Equation 4 such that,

$$r_a(eq) = 0.282 \cdot \sqrt{A_a} \ . \qquad (12$$

Potential of the pipe at $z=r_a(eq)$ was then taken as f_a. Figure 2 shows potential attenuation plots, as determined from Equation 11, in comparison to results acquired using Boundary Element Modeling and Equation 6 for the pipe, cp, and electrolyte parameters listed in Table 2. The trends exhibited here generally conform to those in Figure 1a. The close correspondence between results for the first two methods confirms accuracy of Equation 11 since, for such a small L_{as}, $R_m \rightarrow 0$. Accuracy can also be confirmed by an independent calculation of $I_a \cdot R_a$, which yields the potential difference between the anode and pipe (f_c - f_a). Obviously, the solution of Equation 6 provides poor correlation except at $a \cdot g$ = 1,000 Ωm^2, because of it not incorporating anode resistance.

An example where metallic path resistance is not expected to be negligible was also analyzed based upon the same parameters as in Table 2 for $a \cdot g$ = 100 Ω·m^2 but with L_{as} = 6,000 m [7]. Figure 3 shows the calculated potential profile for cases of r_m = 0 and $1.70 \cdot 10^{-7}$ Ω·m. An independent calculation of anode voltage drop, Df_a, was made using the equation,

$$I_a \cdot R_{r_a \rightarrow z} = \frac{I_a \cdot r_e}{4 \cdot p \cdot r_a}, \qquad (13$$

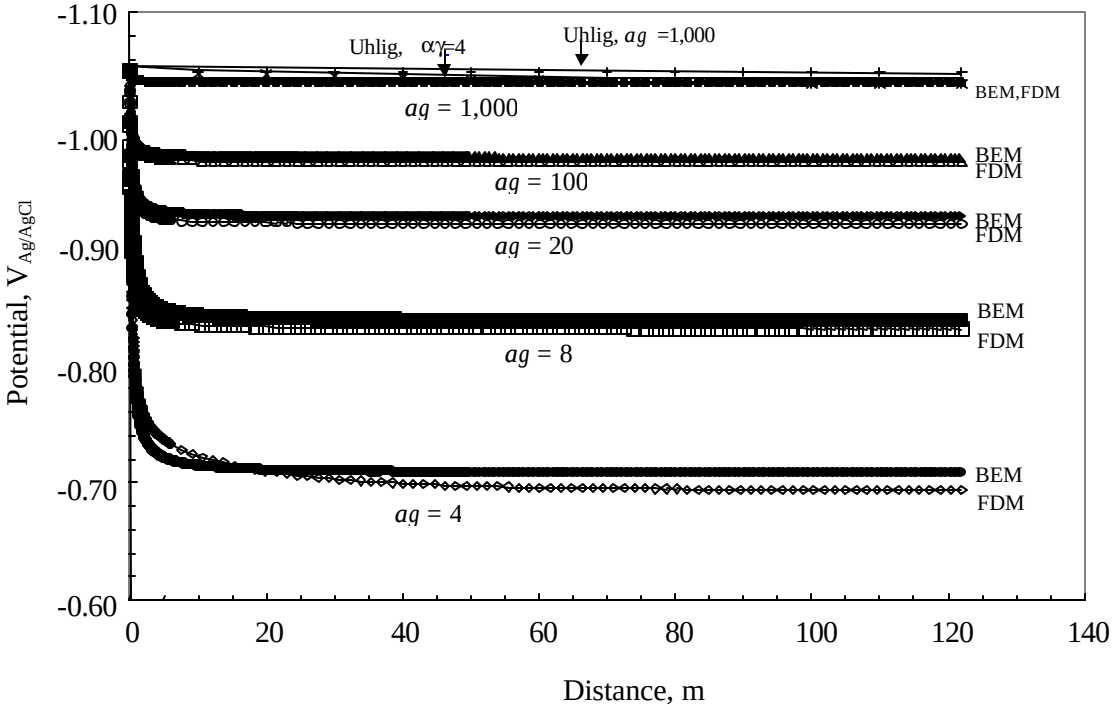

Figure 2: Comparison of attenuation curves as determined from a COMB-FDM solution to Equation 11, BEM, and Equation 6. (Note: the FDM curves were determined using an earlier version of Equation 11 [7]. The difference between these results and ones from Equation 11 is small for the pipe parameters assumed).

Table 2: Pipe, cp, and electrolyte parameters for the attenuation profiles in Figure 2.

Pipe Outer Radius, m	0.1355
Pipe Inner Radius, m	0.1280
Anode Spacing, m	244
Anode Radius, m	0.187
Anode Length, m	0.432
Equivalent Spherical Anode Radius, m	0.201
Anode Potential, $V_{Ag/AgCl}$	-1.05
Pipe Corrosion Potential, $V_{Ag/AgCl}$	-0.65
Electrolyte Resistivity, Ω·m	0.30
Metallic Resistivity, Ω·m	1.70E-07

where r_a is radius of the spherical anode (0.201 m) and I_a was determined as 2.654 A by numerically integrating the area under the f_c-z curve. This yielded 0.315 V; and from this a corresponding far field pipe potential of -0.735 $V_{Ag/AgCl}$ was calculated. Also, f_c was estimated as the breakpoint in the 'w/ pipe resistance' curve in Figure 3 as -0.73 $V_{Ag/AgCl}$, whereas the actual data showed potential at z = 15 m (at this distance f_c was changing at less than one mV per 10 m) as -0.737 $V_{Ag/AgCl}$. Figure 4 shows the more positive potential portion of the w/ pipe resistance attenuation curve in Figure 3 along with a second curve based upon Equation 6 with the drainage point potential set equal to -0.735 $V_{Ag/AgCl}$. This latter curve superimposes upon the COMB-FDM one in the R_m dominated region with the far-field potential between the two methods differing by only two mV.

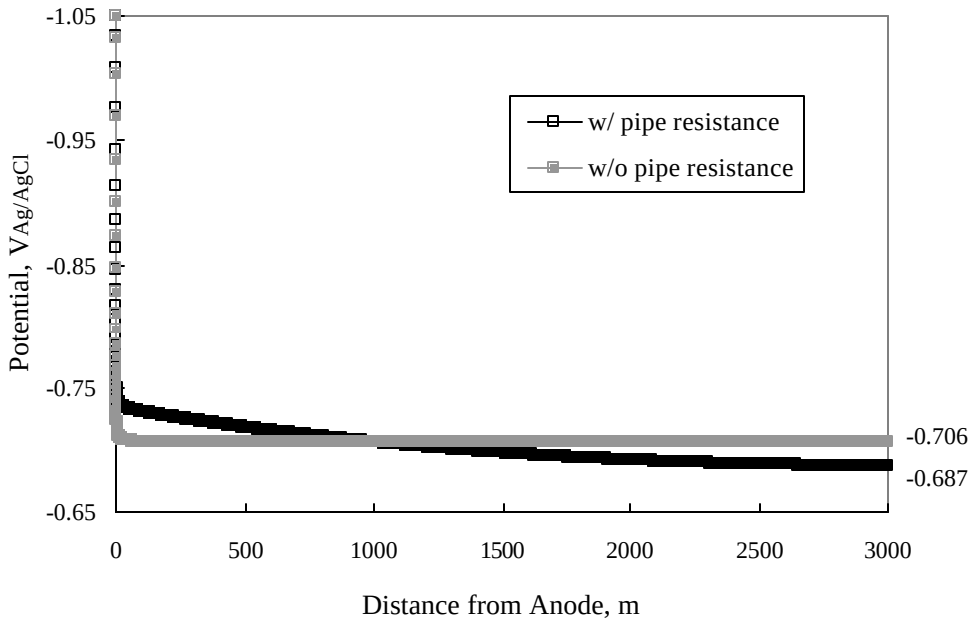

Figure 3: FDM solutions to Equation 11 with presence and absence of the metallic path resistance term.

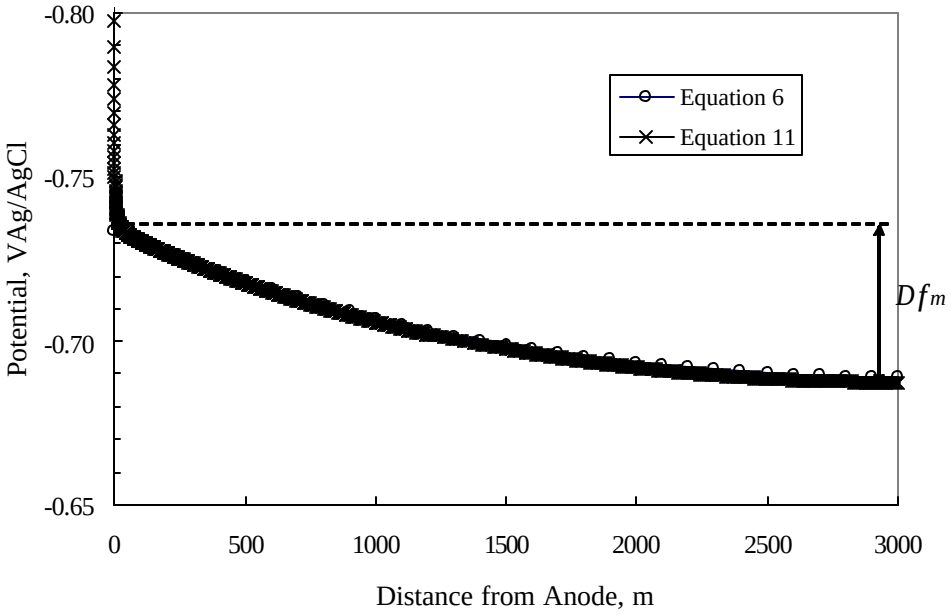

Figure 4: Comparison of the R_m dominated portion of the attenuation equation in Figure 3 (Equation 11) and the solution of Equation 6 with drainage point potential for the latter equal to f_c just beyond the anode potential field.

Pipelines Protected by Displaced Anodes: The case of pipelines protected by identical, equally spaced displaced (offset) anodes has also been analyzed [8]. This involved a modification of the protocol utilized for derivation of Equation 11 based upon the arrangement and terms illustrated schematically in Figure 5 and substitution into Equation 8 the expressions,

$$I_e(z) \equiv 2 \cdot \int_z^L 2 \cdot p \cdot r_p \cdot i_c(t) \cdot dt = \frac{4 \cdot p \cdot r_p}{a \cdot g} \cdot \int_z^L E(t) \cdot dt \quad \text{and} \qquad (14$$

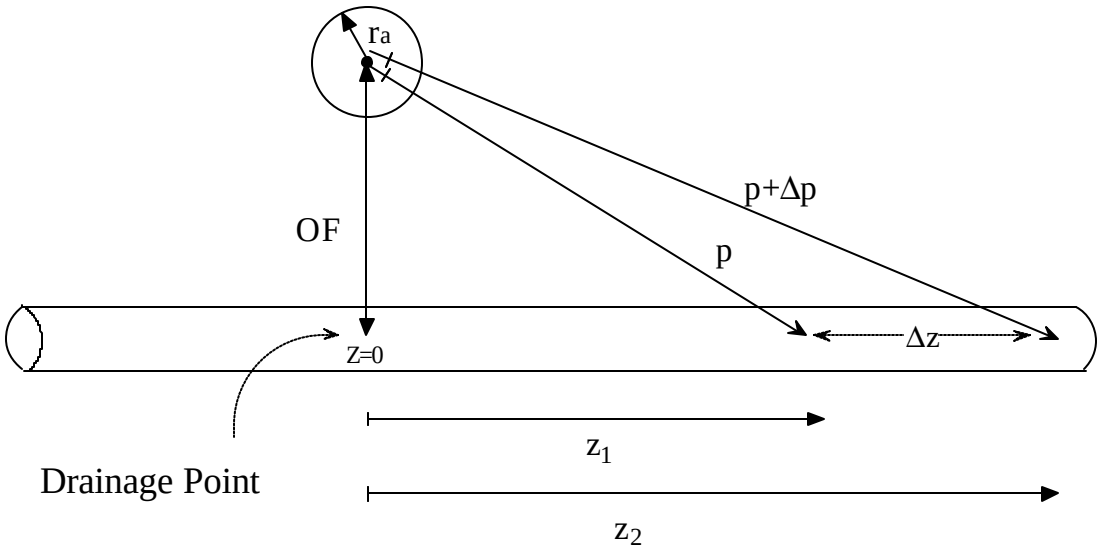

Figure 5: Schematic illustration of assumed arrangement between an offset anode and pipeline.

$$\Delta R_e = \frac{r_e}{4 \cdot p \cdot p}\left[1-(1-\left(\frac{\Delta p}{p}\right)+\left(\frac{\Delta p}{p}\right)^2-\left(\frac{\Delta p}{p}\right)^3 \ldots)\right], \qquad (15$$

where $p \equiv \sqrt{z^2 + OF^2}$ with *OF* being defined in Figure 5. With appropriate manipulations and substitutions, Equation 7 becomes,

$$E_c''(z)+\left(B+\frac{H \cdot z}{\left(z^2+OF^2\right)^{3/2}}\right) \cdot E_c(z) = -H \cdot Q \cdot \int_z^{L_{as}/2} E(t) \cdot dt, \qquad (16$$

where $Q = \left[\frac{1}{\left(z^2+OF^2\right)^{3/2}} - \frac{3 \cdot z^2}{\left(z^2+OF^2\right)^{5/2}}\right]$.

Using an offset distance (*OF*) of zero, which is synonymous with the anode being superimposed, it can be shown that Equation 16 reduces to Equation 11. Thus, Equation 16 encompasses Equation 11 and is proposed as a more general expression, based on first principles, for pipelines protected by identical, evenly-spaced, equally displaced anodes.

Solutions to Equation 16 were obtained using the same CoMB-FDM numerical procedure as for Equation 11. As was the case for Equation 11, Equation 16 was derived assuming gacp. Greater applicability of Equation 16 is likely to result, however, with adaptation for pipelines with iccp systems. This can be accomplished in terms of an equivalent galvanic anode with potential $f_a(eq)$ that provides the same polarization as the ic one, as defined by the expression [9],

$$V = f_a(ic) - f_a(eq), \qquad (17$$

where *V* is the rectifier voltage and $f_a(ic)$ is potential of the ic anode. An example based upon the above equations was developed assuming a rectifier voltage of 10 V, an ic anode potential of 1.50 V_{CSE}, with other parameters as listed in Table 3. The unrealistically large anode (0.374 m radius and 2.677 m long) is intended to

be equivalent resistance-wise to a multiple anode array. As above, $r_{a(eq)}$ was calculated using Equation 12. Knowing $f_a(eq)$ and $r_a(eq)$, the equivalent spherical anode was superimposed on the pipeline; and potential at the first node was set equal to $f_a(eq)$. The total anode output current, I_A, was then numerically calculated from the potential profile generated from the CoMB-FDM based FORTRAN program. This current was used to calculate the drainage point potential, f_{dp}, according to the expression,

$$f_{dp} = f_a(eq) + I_A \cdot R_{r_a(eq)\to OF} = f_a(eq) + \frac{I_A \cdot r_e}{4p}\left[\frac{1}{r_{a(eq)}} - \frac{1}{OF}\right]. \qquad (18$$

Table 3: Assumed pipe, cp, electrolyte parameters.

Pipe Outer Radius, m	0.136
Pipe Inner Radius, m	0.128
Anode Spacing, m	100,000
Anode Radius, m	0.374
Anode Length, m	2.677
Equivalent Spherical Anode Radius, m	0.749
Anode Offset Distance, m	25, 100, 500
Polarization Resistance, a, $\Omega\cdot m^2$	17.5
Pipe bare area, percent	0.1
Corresponding, $a'g$, $\Omega\cdot m^2$	17,500
Pipe Corrosion Potential, V_{CSE}	-0.30
Electrolyte Resistivity, $\Omega\cdot m^2$	100
Metallic Resistivity, $\Omega\cdot m^2$	1.70E-07

Figure 6 shows a plot of f_c versus z for the parameters in Table 3 based upon the procedure outlined above in conjunction with both Equations 16 and 6. In each case, f_c is projected to be more positive based upon the former than the latter with the difference being relatively large for OF = 25 m and negligible for 500 m. This difference is expected to increase also with increasing electrolyte resistivity (constant current density demand) and $a'g$. Clearly, the anode potential field is influential at the smaller OF values such that the Equation 6 projections are non-conservative. Figure 7 illustrates these same plots on a semilog scale such that the distinction between the Equation 16 and 6 results is more apparent. The finding that the potential profiles projected by both approaches essentially superimpose for the case where the pipeline is beyond the anode field (OF = 500 m) constitutes additional confirmation of Equation 16.

An alternative approach is illustrated in Figure 8, where again projections were developed using Equations 6 and 16 for the same parameters as in Table 3 but with OF = 25 m and L_{as} values of 25, 50, and 100 km. In this case, f_{dp} for application of Equation 16 was based upon Equation 18, as before; however, f_{dp} for Equation 6 utilized the expression,

$$f_{dp} = f_a(eq) + \frac{I_A \cdot r_e}{4p}\left[\frac{1}{r_{a(eq)}}\right]. \qquad (19$$

As such, the Equation 6 attenuation curves neglect completely the anode potential field. Table 4 lists the f_{dp} and mid-anode spacing potentials for each of the three examples according to both equations. Because for the

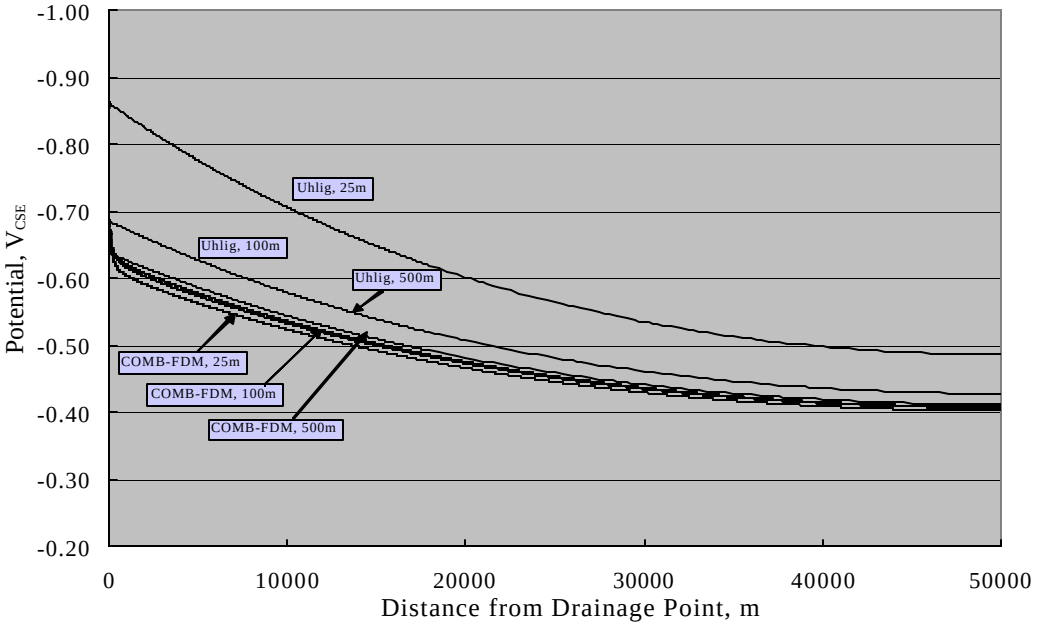

Figure 6: Potential profiles for the pipe, cp, and electrolyte parameters listed above and in Table 3 according to Equations 16 and 6.

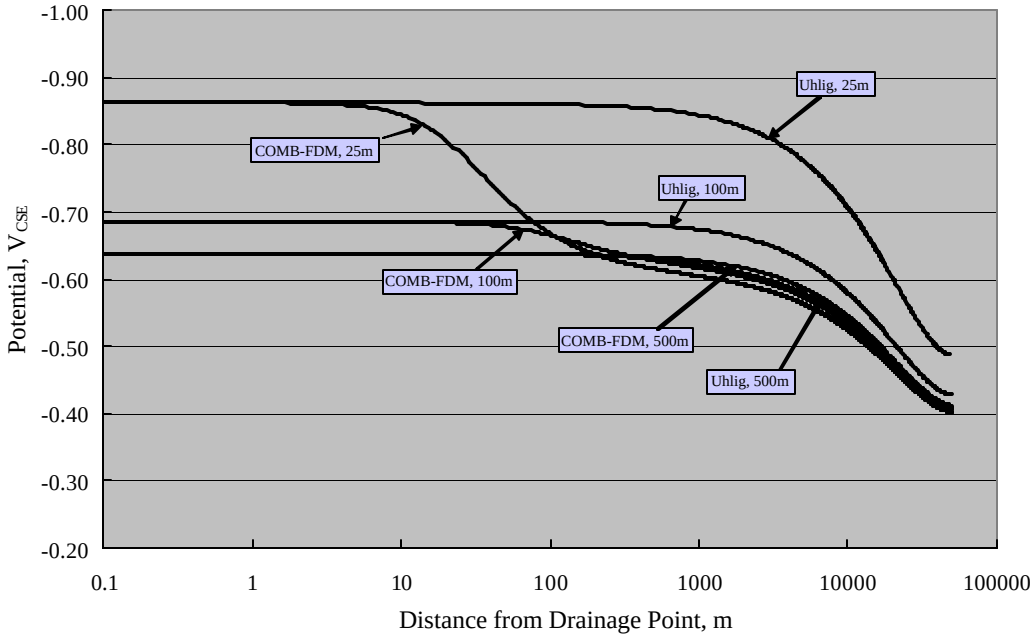

Figure 7: Representation of the Figure 6 data in semilog format.

relatively small *OF* employed here a portion of the pipeline is within the anode potential field, f_{dp} is consistently more negative based upon Equation 18 than Equation 19. The mid-anode potentials, on the other hand, are in good mutual agreement (maximum difference 8 mV).

In Figure 9, the profiles from Figure 8 are shown in semilog format. The purpose for doing this is to emphasize the near field, where potentials projected by the two methods remain different. Thus, at 100 m, the potential projected by Equation 6 is approximately 50 mV more positive than for Equation 16, whereas within 10

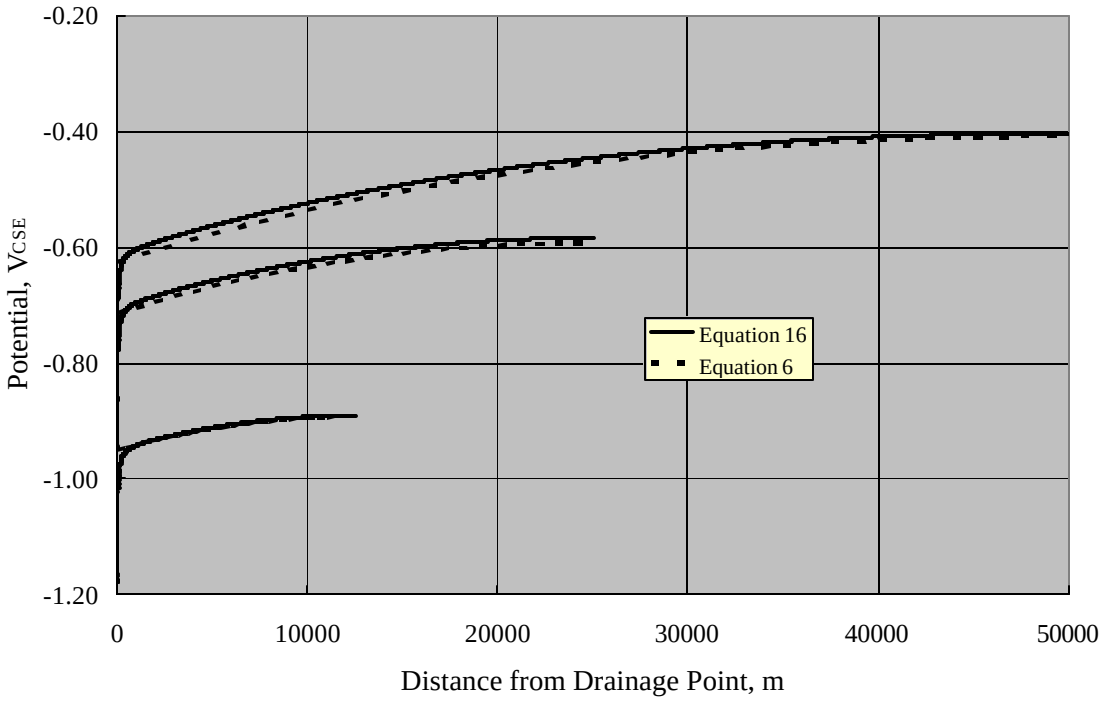

Figure 8: Potential profiles based upon Equations 6 and 16 for the parameters in Table 3 and the f_{dp} values in Table 4.

Table 4: Comparison of drainage point and mid-anode spacing potentials for the example in Figure 8.

	Equation 16		Equation 6	
Anode Spacing , m	f_{dp}, V_{CSE}	f_c(Las/2), V_{CSE}	f_{dp}, V_{CSE}	f_c(Las/2), V_{CSE}
25000	-1.177	-0.890	-0.951	-0.892
50000	-0.947	-0.584	-0.714	-0.592
100000	-0.862	-0.403	-0.627	-0.408

m of the drainage point this difference exceeds 200 mV. While this difference does not pose a corrosion risk, it could contribute to coating damage or hydrogen embrittlement (or both).

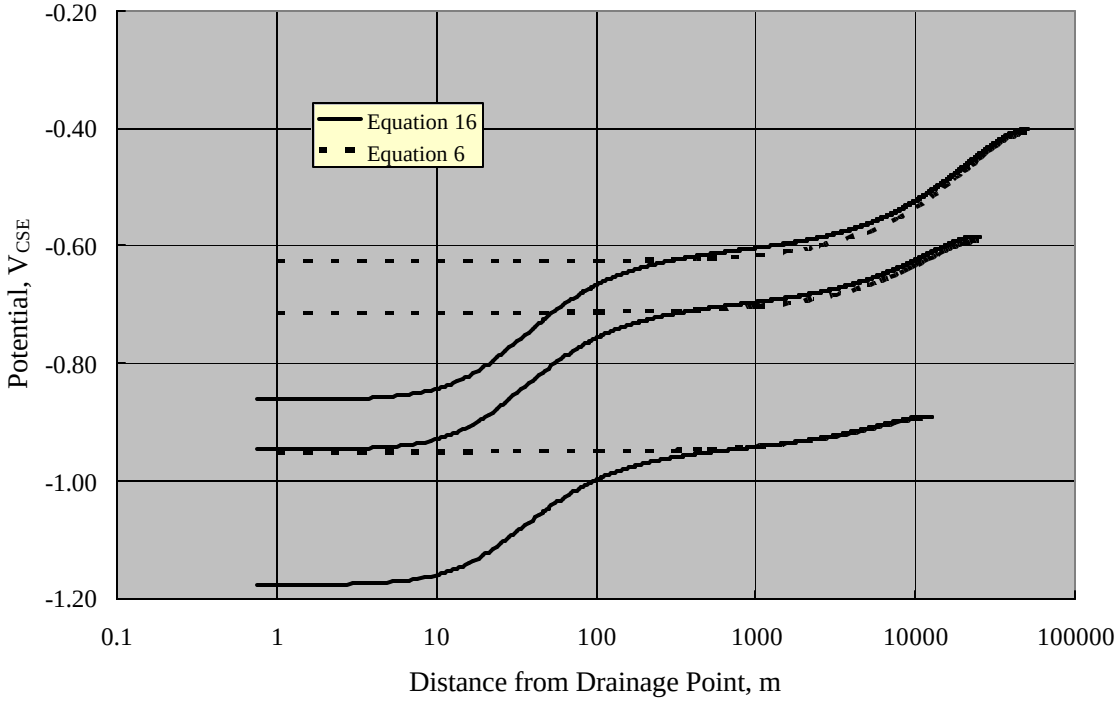

Figure 9: Representation of the Figure 8 data in semilog format.

Conclusions

The newly proposed potential attenuation equation for cathodically polarized pipelines and risers with identical, equally spaced anodes has been derived as,

$$E_c''(z)+\left(B+\frac{H\cdot z}{\left(z^2+OF^2\right)^{3/2}}\right)\cdot E_c(z)=-H\cdot Q\cdot\int_z^{L_{as}/2}E(t)\cdot dt\,,$$

where

$E_c(z)$ is the magnitude of polarization as a function of distance z from an anode,

$$H=\frac{r_e\cdot r_p}{a\cdot g}\,,$$

$$B=\frac{-R_m\cdot 2\cdot p\cdot r_p}{a\cdot g}\,,$$

L_{as} is anode spacing,
r_e is electrolyte resistivity,
r_p is outer pipe radius,
R_m is pipe resistance per unit length,
a is polarization resistance,
g is ratio of total pipe surface area to bare surface area,
OF is anode offset distance, and

$$Q=\left[\frac{1}{\left(z^2+OF^2\right)^{3/2}}-\frac{3\cdot z^2}{\left(z^2+OF^2\right)^{5/2}}\right].$$

For the case of superimposed anodes ($OF = 0$), as occurs for bracelet anodes on marine pipelines, the expression reduces to,

$$E''(z)+\left(\frac{H}{z^2}+B\right)\cdot E(z)=\frac{2\cdot H}{z^3}\int_z^{L_{as}/2}E(t)\cdot dt\,.$$

Accuracy of both equations is demonstrated, and example analyses are provided. The results indicate that these two expressions are in good agreement with the classical equations of Morgan and Uhlig when the pipe is beyond the anode potential field and that they provide improved accuracy in potential attenuation projection compared to the Morgan and Uhlig expressions in cases where the pipeline or a portion thereof lies within the anode potential field.

Acknowledgements

The authors are indebted to member organizations of a joint industry project, including ChevronTexaco, ExxonMobil, Shell Pipeline Company, and the Minerals Management Service for financial sponsorship of this research.

References

1. "Cathodic Protection Design," *DnV Recommended Practice RP401*, Det Norske Veritas Industri Norge AS, 1993.

2. "Pipeline Cathodic Protection – Part 2: Cathodic Protection of Offshore Pipelines," Working Document ISO/TC 67/SC 2 NP 14489, International Standards Organization, May 1, 1999.

3 McCoy, J.E., The Institute of Marine Engineers Transactions, Vol. 82, 1970, p. 210.

4. Morgan, J., *Cathodic Protection*, Macmillan, New York, 1960, pp. 140-143.

5. Uhlig, H. H. and Revie, R. W., Corrosion and Corrosion Control, Third Ed., J Wiley and Sons, New York, 1985, pp. 421-423.

6. Pierson, P., Bethune, K., Hartt, W. H., and Anathakrishnan, P., Corrosion, Vol. 56, 2000, p. 350.

7. Lysogorski, D.K., Hartt, W.H., and Ananthakrishnan, P. "A Modified Potential Attenuation Equation for Cathodically Polarized Marine Pipelines and Risers," paper no. 03077 to be presented at CORROSION/03. To be published in *Corrosion.*

8. Lysogorski, D.K. and Hartt, W.H., "A Potential Attenuation Equation for Design and Analysis of Pipeline Cathodic Protection Systems with Displaced Anodes," paper no. 03196 to be presented at CORROSION/03, March 16-21, 2003, San Diego.

9. Hartt, W.H., "The Slope Parameter Approach to Marine Cathodic Protection Design and Its Application to Impressed Current Systems," in Designing Cathodic Protection Systems for Marine Structures and Vehicles, Ed. H. Hack, Special Technical Publication 1370, Am. Soc. For Testing and Materials, West Conshohocken, PA, 1999.